



Self-Sealing Polyolefin by Super-Absorbent Polymer

He Zhang,^{1,2*} Yong Bing Chong,² Ying Zhao,³ Andrey Buryak,⁴ Fei Duan^{2*} and Jinglei Yang^{2,3*}

In this study, self-sealing polyethylene (PE) was successfully achieved *via* incorporating super-absorbent polymer (SAP). Attributed to the high thermal stability, the SAP particles can survive through the harsh processing conditions during thermal extrusion and hot pressing. PE specimens with different concentrations of SAP particles of different sizes show good sealability with fast response to water penetration through pin-hole and crack defects. It was observed that a higher concentration of smaller SAP particles enables better sealing performance under normal pressure. Additionally, repeated sealing can be achieved with full sealability due to the left SAP residue from the last cycle in the defects.

Keywords: Self-sealing; Super-absorbent polymer (SAP); Water penetration; Water absorption; Thermal processing

Received 3 April 2019, **Accepted** 25 June 2019

DOI: 10.30919/es8d801

1. Introduction

Self-healing of material cannot only fill and seal defects in matrix, but also restore their lost or degraded mechanical properties.^{1,3} In order to achieve high healing performance, stringent requirements must be met since chemical reactions under specific conditions are necessary in most cases. However, under certain circumstances, mechanical properties of matrix are not the main consideration whereas the re-establishment of other properties, such as the self-sealing property, is of great and practical significance to retard or even impede penetration of fluids like water or gases. One typical example is the self-healing of functional coatings.^{4,5} Because anticorrosion is the main purpose of the protective coating, the re-establishment of mechanical properties is not important and less concerned. Lots of efforts have been made into this direction in the self-healing area and diversified self-healing systems were explored to achieve this function.^{6,9} And in some other cases, self-sealing composites were developed to impede the diffusion or penetration of pressurized gases after damaging event.¹⁰⁻¹²

As can be seen in most systems, microcapsules containing reactive monomers were fabricated and mixed into the matrices to realize the self-healing/self-sealing functionality through chemical reactions.¹³⁻¹⁶ However, the introduction of self-sealing functionality by incorporating microcapsules has its own limitations. Firstly, when they are

incorporated into other matrices, the microcapsules with the liquid core can be taken as defects, which significantly compromises the original mechanical properties of the matrix. This is an unavoidable shortcoming and has been repeatedly criticized for almost all the functionalized systems by the introduction of microcapsules.¹⁷⁻¹⁹ Secondly, the introduction of reactive liquids, such as isocyanate, might cause some safety related issues, such as toxicity.^{20,21} The safety issues may eventually halt the commercialization of the system. Thirdly, self-sealing based on encapsulated reactive sealants can only seal defect for one time. Since chemical reaction for the released healants from microcapsules is irreversible, repeated sealing of the same location is impossible. Fourthly, the long-term and thermal stability of the reactive sealants is also a big issue, especially when thermal treatment is necessary during processing of the material and thermal shocks appear frequently during servicing of the material. Additionally, when comes to thermoplastics, the weak microcapsules are unable to survive through the harsh processing conditions with high temperature, high pressure, and high shear stress. Finally, the high cost, introduced by both the raw material, i.e. reactive sealants, and the encapsulation process, lays the potential limit for commercialization.

According to previous research, most of the self-healing/self-sealing systems were developed in thermosets, because incorporation of microcapsules into a thermosetting matrix which is resulted from liquid monomers is much easier.^{22,23} However, due to the wider range of sources and lower cost as compared to the thermosets, thermoplastics are more widely used in daily life and industry. Consequently, self-healing/self-sealing in thermoplastics is also important, considering their huge consumption and vulnerability to external forces. Nevertheless, self-healing/self-sealing in thermoplastics progresses slowly, attributed to the survivability of healing agent carriers through the harsh processing conditions for thermoplastics. Although relatively high healing performance was achieved in some thermoplastics by incorporation of microcapsules, the preparation methods for the specimens are non-mainstream for thermoplastics in order to guarantee the survivability of the carriers.²⁴⁻²⁶ Besides this, other issues introduced by the incorporation of microcapsule as mentioned above also exist for those systems. In order to explore the self-healing/self-sealing

¹ The National Engineering Research Center of Novel Equipment for Polymer Processing, The Key Laboratory of Polymer Processing Engineering (SCUT), Ministry of Education, South China University of Technology, Guangzhou, China, 510641

² School of Mechanical and Aerospace Engineering, Nanyang Technological University, 639798, Singapore

³ Department of Mechanical and Aerospace Engineering, The Hong Kong University of Science and Technology, Kowloon, Hong Kong SAR, China

⁴ Borouge PTE, Borouge Innovation center, Sas Al Nakhl, Abu Dhabi, UAE

*E-mail: zhanghe@scut.edu.cn; feiduan@ntu.edu.sg; maeyang@ust.hk

functionality in thermoplastics, other sealants/sealants with higher mechanical and thermal stability should be explored.

Super absorbent polymer (SAP) is a class of lightly cross-linked hydrophilic polymer which can absorb and retain extremely large amount of water or aqueous solutions through hydrogen bonding with water molecules.²⁷ Attributed to the relatively low price, low toxicity, and the unique feature that can absorb huge amount of water, it has been commercialized and widely applied in hygienic needs, environmental control and protection, agriculture and horticulture, pharmaceuticals, *etc.*²⁷ Recently, other potential applications were also explored based on the unique properties of SAP.²⁸⁻³¹ Besides being used to retain water in concrete to control the hardening process to achieve higher property of hardened concrete,³²⁻³⁴ it is also adopted as *in-situ* sealant to seal cracks in concrete to avoid water penetration.^{30, 31} Due to high absorbability of water, it can effectively retard or even completely impede penetration of water through the cracks in concrete. During the self-sealing process, it responds rapidly upon contacting with water to swell and block cracks. Because the absorption and desorption of water is a reversible physical process, multiple sealing cycles can be achieved for the same defective area. However, when it is used as a sealant in concrete, it also encounters some problems because of the mutual influence between concrete and SAP. On one hand, the incorporated SAP affects the hardening process of the concrete and may leave a huge amount of voids after the SAP particles shrink by desorbing the water which is absorbed during the hardening process of concrete. On the other hand, the concrete itself seriously influence the swellability of the incorporated SAP particles. The swelling of SAP is not only very sensitive to pH and ionic strength of the solution, but also the type of ions present in the solution.³⁵ In particular, the presence of bivalent cations has a large effect on absorption capacity and this could limit the application of SAP as fluid barrier.³⁶ Although modified SAP with higher resistance to pH and ionic strength was achieved, it inevitably increases the cost for practical commercialization.^{37, 38}

Considering the high swellability, good mechanical property as a solid particle and high thermal stability, SAP has the potential to be used to realize self-sealing in thermoplastics. In this investigation, the feasibility of SAP as sealants for thermoplastics, i.e. polyethylene (PE), was explored. Firstly, the basic properties of the adopted SAP were studied in terms of the maximum absorbability of water, thermal stability, and survivability through thermal processes. And then, the sealability of SAP to the defects in PE was tested under both normal pressure and extra pressure.

2. Experimental section

2.1 Materials

SAP based on cross-linked sodium poly(acrylate) was purchased from Sigma-Aldrich (Singapore). PE, with commercial name MB6561, was provided by Borouge Pte Ltd.

2.2 Granulation of SAP

The original SAP, with a particle size up to 850 μm , was granulated to smaller particles using a dry grinding method. Firstly, the mortar, pestle, and original SAP were dried at 80 °C under high vacuum in an oven (Binder, Model V53) for about 12 h to completely remove the absorbed moisture. Then in the same oven with a temperature of 80 °C, the dried original SAP particles were granulated to small SAP particles for about 30 min. Finally, the granule SAP particles were sieved in the oven to achieve particles with size ranges of 38-180 μm (small) and 180-300 μm (big). The sieved SAP particles were stored in sealed vials for further usage.

2.3 Water absorption test of SAP particles in water

The maximum absorbability of SAP particles was firstly studied by immersing about 1.0 g SAP particles in an excessive amount of water (about 1.0 L). The SAP particles turned to SAP gels immediately when they got in contact with water. After about 10min when the SAP particles were completely saturated with water, the swollen SAP gels were separated by firstly filtrating and then absorbing the residual free water around by tissue. The weight was recorded for calculation of the maximum absorbability. Influence of repeated cycles on maximum absorbability was conducted by desorbing the water in SAP gels completely at 80 °C for 24 h, and then re-absorbing water again. About 10 cycles were carried out to investigate the reversibility of this process. In order to obtain average value with standard deviation (SD), three independent measurements were carried out based on three replicates.

2.4 Moisture absorption of SAP particles in open air

Because SAP based on sodium poly(acrylate) has a high affinity with water, it can also absorb the moisture in the surroundings. The maximum absorbability in the open air, i.e. room temperature (RT ~22-25 °C) and relative humidity of 80%, was conducted by spreading about 1.0 g SAP particles on an aluminum foil and recording the weight change with respect to time. Three independent measurements were carried out based on three replicates to obtain average value with SD.

2.5 Survivability of SAP particles through thermal processes

Firstly, the survivability of the adopted SAP through thermal processes was studied. For this testing, the mixture of PE, i.e. MB6561, and SAP particles was subjected to thermal extrusion and hot pressing. The granulated SAP particles with a size in 38-180 μm and 180-300 μm were firstly mixed with MB6561 powder at concentrations of 5 wt% and 10 wt%, and dried at 80 °C under vacuum for about 12 h (Binder, Model V53). 5.0 g of the mixture was fed into a mini-extruder (Haake Minilab II) and processed at 180 °C with a rolling speed of 60 round/min for 10min. The survivability of SAP particles through hot-press processing was conducted by subjecting the above-mentioned dry mixture to a hot press (CARVER). The mixture (about 25.0 g) in a mold with a chamber size of 100*100*2 mm^3 was firstly melted at 180 °C for about 20 min, then pressed by a load of 6.0 ton at 180 °C for about 10min, and finally cooled down in the hot press to 100 °C after shutting off the heat source.

2.6 Fabrication of self-sealing PE

Specimens for self-sealing testing, including both pure and self-sealing PE plates, were prepared by hot pressing using the processing condition as mentioned above. All the specimens were cut into small pieces with a dimension of 50*50*2 mm^3 for a water penetration test. Table 1 shows information for the prepared specimens. In order to minimize the water absorption by the dispersed SAP particles near the surface, all the specimens, including the pure PE and self-sealing PE, were coated with a thin layer of UV curable resin (NOA 61, Edmunds).

2.7 Water penetration test

Water penetration test was carried out using a device as shown in Fig. 1a. It consists of a water container, a clamp with an adjustable screw to ensure water tightness, a rubber O-ring for better sealability between the water container and the testing specimen, the specimen for testing, and a container for collecting of penetrated water. Before the test, defect in the form of pin-hole was introduced to the center of the specimen by piercing through the specimens using a needle with a diameter of 0.88 mm.

During the tests, 50.0 g water was added into the water container,

Table 1 Specimens prepared by hot pressing.

NO	PROCESSING METHOD	SAP PARTICLE SIZE	SAP CONCENTRATION
		(μm)	(wt%)
#1	Hot pressing	38-180	5.0
#2			10.0
#3		180-300	5.0
#4			10.0

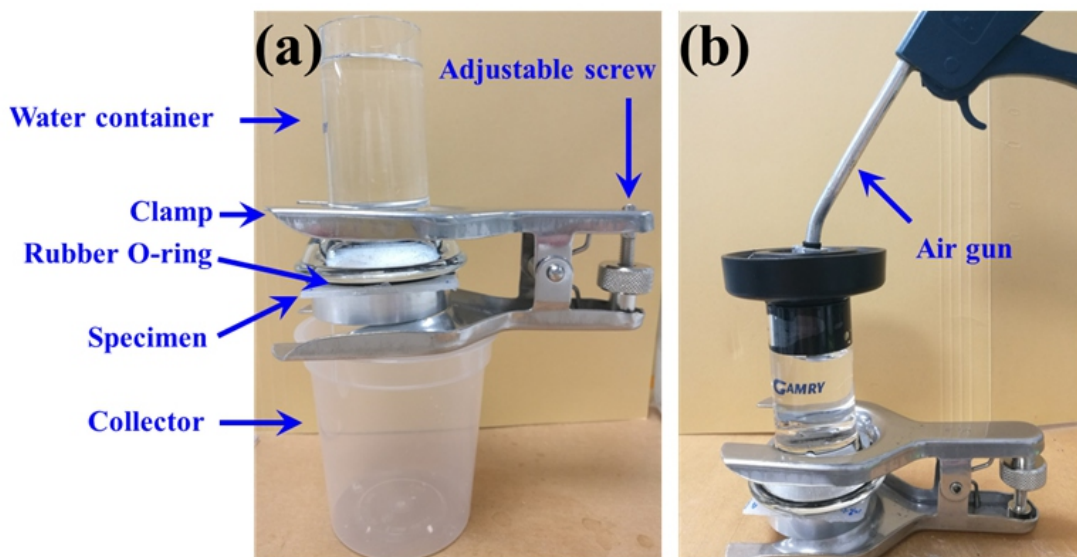


Fig. 1 (a) Setup for water penetration test for PE specimens. It consists of a water container, a clamp with an adjustable screw to ensure tightness, a rubber O-ring for better sealability between the water container and testing specimen, the testing specimen, and a container to collect the penetrated water; (b) Setup for water penetration test under elevated pressure. Extra pressure can be controlled and adjusted by the air gun.

Table 2 Specimen information and cycling test on self-sealing specimens with defect in form of pin-hole for a water penetration test.

NO.	SIZE (μm)	CON. (wt%)	CYCLE 1 (g)	CYCLE 2 (g)	CYCLE 3 (g)	CYCLE 4 (g)	CYCLE 5 (g)	CYCLE 6 (g)
#1	0	0	26.1 \pm 3.1	NA	NA	NA	NA	NA
#2	38-180	5.0	1.8 \pm 0.6 ^a	0	0	0	0	0
#3		10.0	0.55 \pm 0.23	0	0	0	0	0
#4	180-300	5.0	2.7 \pm 0.8	0	0	0	0	0
#5		10.0	1.0 \pm 0.4	0	0	0	0	0

^a The last drop falls off at around 20-40s

and the penetrated water through the pin-hole was recorded regarding the penetrating duration. All the penetration tests lasted for 8 min to make sure that the water in the container did not penetrate any more. In order to test the cycling performance for the self-sealing specimens, the tested specimens were dried at 80 °C for about 12 h and subjected to the same procedure. The specific sample information can be found in Table 2.

Water penetration test of the self-sealing specimens with a defect in the form of crack was also investigated. Cracks with different lengths and widths were introduced to the self-sealing specimens with 10 wt% small SAP particles (38-180 μm) by cutting with a sharp blade. The testing procedure is the same as that mentioned above, and the specific sample information can be found in Table 3.

Water penetration tests with the presence of extra pressure were

conducted on self-sealing specimens using a device as shown in Fig. 1b. An air gun with adjustable pressure was introduced to the test setup. The sample information and testing condition were given in Table 4. An extra pressure of 3psi (20.68 kPa) was exerted to self-sealing specimens with 10 wt% small SAP particles (38-180 μm), while extra pressure from 3 psi (20.68 kPa) to 6 psi (41.36 kPa) was exerted to self-sealing specimens with 10 wt% big SAP particles (180-300 μm).

2.8 Characterization

The thermal stability of the original SAP was characterized by thermogravimetric analysis (TGA, AutoTGA Q500). In TGA test, 10-30mg sample was charged into a platinum pan and heated under designated atmosphere (air or N_2) with a ramp rate of 10°C/min. The fractured surface was observed using a field emission scanning

Table 3 Specimen information and cycling test on specimens with defect in form of crack for a water penetration test.

NO.	SAP SIZE (μm)	SAP CON. (wt%)	CRACK LENGTH (mm)	CRACK WIDTH (μm)	CYCLE #1 (g)	CYCLE #2 (g)	CYCLE #3 (g)
#1	0	0	10	129 \pm 13	37.5 \pm 4.7	NA	NA
#2	38-180	10.0	10	138 \pm 11	0	0	0
#3	38-180	10.0	20	217 \pm 15	3.2 \pm 1.3	0	0

Table 4 Specimen information and parameter for water penetration testing with extra pressure.

NO.	SAP SIZE (μm)	SAP CON. (wt%)	EXTRA PRESSURE (psi/kPa)
#1	38-180	10.0	3/20.68
#2	180-300	10.0	3-6/20.68 -41.36

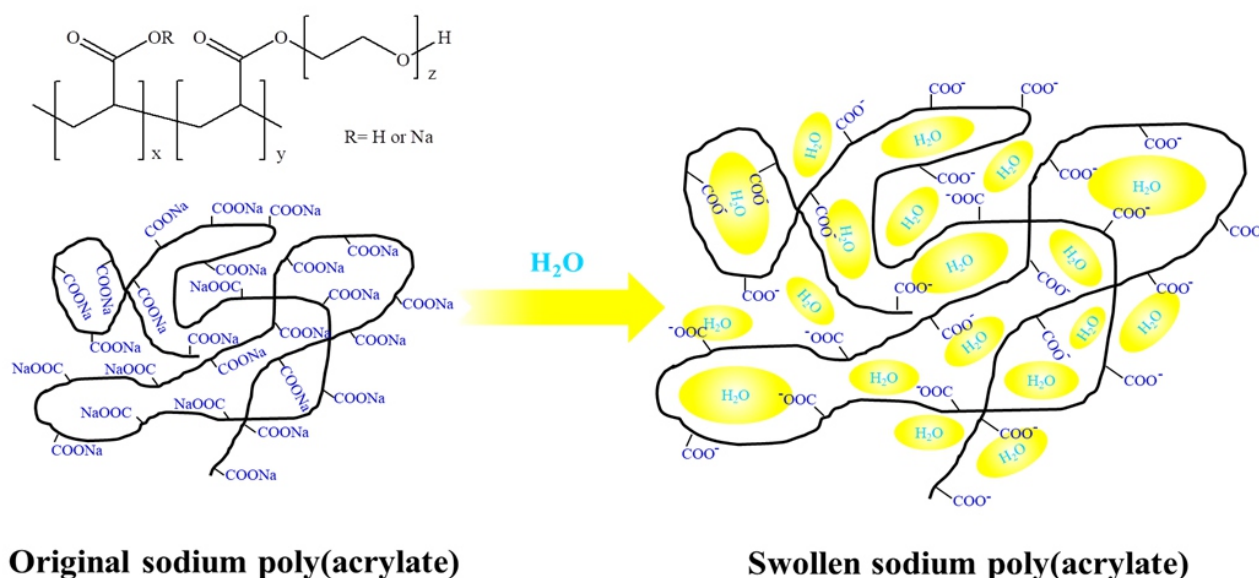


Fig. 2 Schematic molecular structure of SAP based on cross-linked sodium poly(acrylate), and swelling mechanism for the adopted SAP. This SAP has high affinity to water attributed to the $-\text{COONa}$ groups and the polyethylene glycol chain. Due to the low cross-linking density, the polymeric network can only be swollen by the absorbed water rather than dissolved, leading to the rapid and huge volume change.

electronic microscope (FESEM, JOEL JSM-7600F). The defects, in form of either pin-hole or crack, of the fabricated specimens, including pure PE and self-sealing PE, were observed using an optical microscope with transmittance mode.

3. Results and discussion

3.1 Characterization of SAP

3.1.1 Absorbability of SAP in water

In this investigation, the adopted SAP is cross-linked sodium poly(acrylate), which is a lightly cross-linked poly(acrylate) with partial neutralization and partial esterification by poly(ethylene glycol). The molecular structure of this SAP is shown at the top left in Fig. 2. When this kind of polymer gets in contact with water, it can absorb a huge amount of water due to the high affinity of -COONa groups and ethylene glycol groups towards the water. Attributed to the light cross-linkage between different molecules, the polymer can only be swollen, rather than dissolved, by the water around, leading to a huge volume increase of the SAP particles, as schematically illustrated in Fig. 2. After being swollen, the SAP particles hold a huge amount of water firmly and turn to relatively soft and brittle SAP gels.

The maximum absorbability of water for this SAP was studied by immersing the SAP particles in a huge amount of water. It is observed that the SAP particles absorbed water rapidly and arrived the maximum status in less than 2 min. After saturation, the weight of the gel-like solid increases by about $34700 \pm 1800\%$. Since water is only kept in the

polymeric networks by electrostatic force, it can be desorbed gradually when the SAP gels are placed in a dry environment, higher temperature, or vacuum. After being dried, the SAP gels turn to SAP particles again and can absorb water repeatedly. Fig. 3a shows the trend of the maximum absorbability regarding the cycling number. The maximum absorbability decreases dramatically for the 2nd and 3rd cycle to about 80%, relative to the 1st cycle. However, it decreases only slightly thereafter. After about 10 cycles, the remaining absorbability relative to the 1st is about 75%, and the absolute absorbability is more than 25000%, which is still very high. During the absorption of water, the volume of SAP increases dramatically too. However, since it is difficult to quantify it, the volume change was not measured in this investigation.

3.1.2 Absorbability of SAP in open air

Because of the high affinity of this polymer to water, this SAP can also absorb the moisture in the open air. Fig. 3b shows the trend of weight increase with respect to its duration in the open air (RT of $\sim 22\text{--}25^\circ\text{C}$ and relative humidity of about 80%). The absorption of water by the SAP particles is relatively rapid and steady for the first 24 h, but slows down thereafter, and levels off finally. The maximum absorbability is about 75 wt%. After saturation in the open air, the SAP particles turn to elastic and no visible volume change can be observed for the SAP particles, which means it is necessary for the presence of the huge amount of water to trigger the rapid and big volume change of this SAP.

3.1.3 Thermal properties of SAP

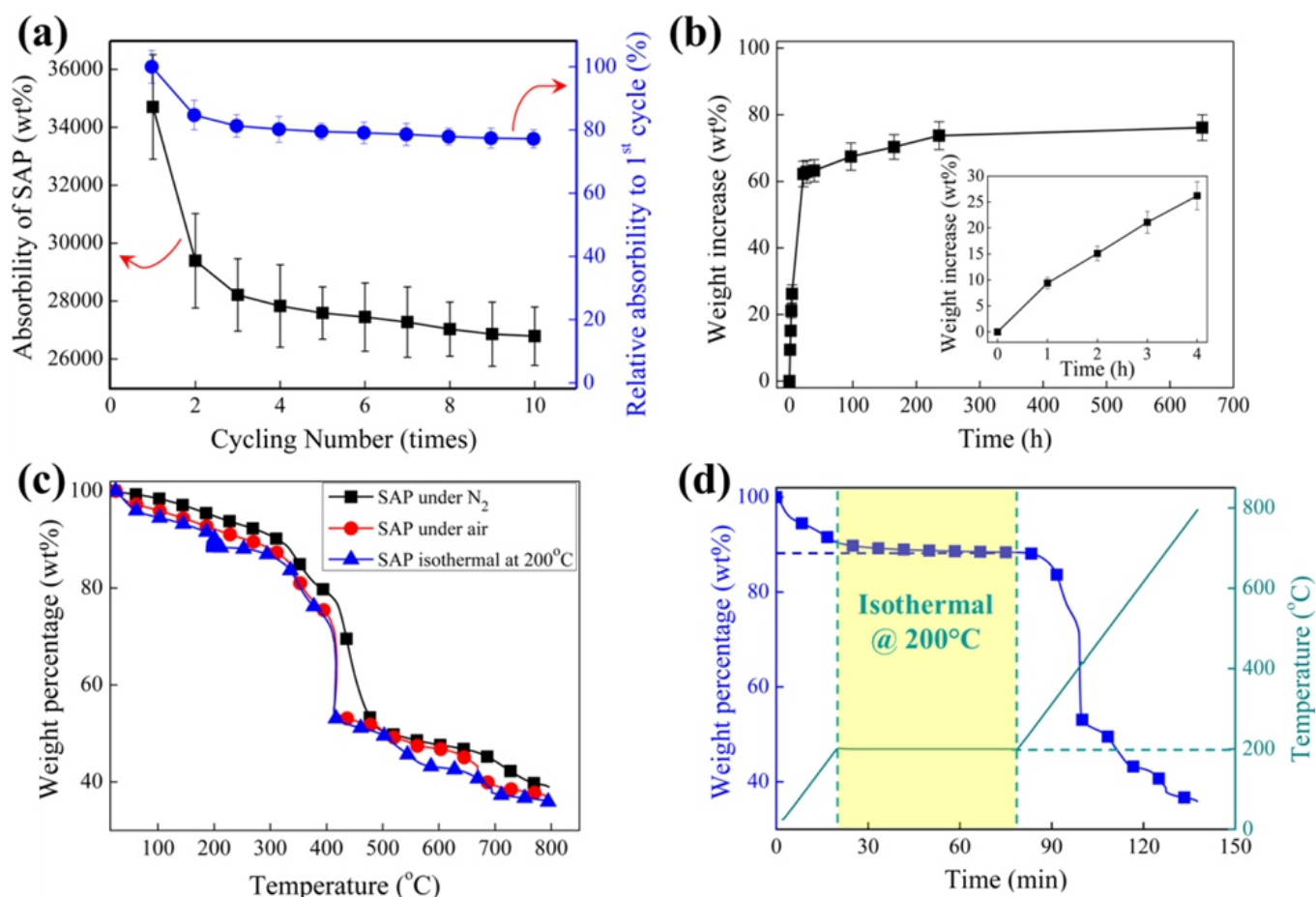


Fig. 3 Basic properties of the adopted SAP based on cross-linked sodium poly(acrylate). (a) Trend of maximum absorbability of the SAP particles with respect to the cycling number when they are immersed in water; (b) Absorption of moisture in open air with respect to time; (c) TGA curves of the SAP particles at atmospheres of air and N_2 to show their thermal stability; and (d) Isothermal treatment at 200°C for 1h for the SAP particles.

As thermal processing is universal and necessary for polyolefins to become the final products, the thermal stability of the adopted SAP at thermal process condition is of great significance to fulfill the self-sealing ability. Fig. 3c gives TGA curves of the SAP with temperature up to 800 °C under both atmospheres of air and N₂. It can be observed that before 300 °C, the SAP decomposes gradually and the weight loss is about 10 wt% under both atmospheres. It shows that the thermal decomposition temperature for this SAP is around 400 °C, which is much higher than the thermal processing condition for most common thermoplastics. As the recommended processing temperature for MB6561 is 160-200 °C, the thermal stability at or before 200 °C is important. Fig. 3d shows the isothermal behavior of this SAP at 200 °C for about 1h. It is found that only about 12 wt% SAP decomposes after the isothermal treatment, which demonstrates good survivability through

the thermal processes for MB6561.

3.2 Survivability of SAP particles through thermal processes

Besides high temperature, other fields, including high pressure and shear stress, exist during thermal processing of thermoplastics. The survivability of SAP particles through the thermal processes, including both extrusion and hot pressing, was investigated by subjecting the mixed SAP particles in MB6561 to a mini-extruder with two counter-rotating screws and a hot press. Fig. 4 shows cross-sections of the fabricated self-sealing specimens with 5 wt% small and big SAP particles by extrusion. Uniformly dispersed SAP particles can be clearly observed for both sizes. Fig. 5 shows SEM images of cross-sections for fabricated self-sealing specimens with 5 wt% small and big SAP particles by hot pressing. Same as that by extrusion, uniformly dispersed

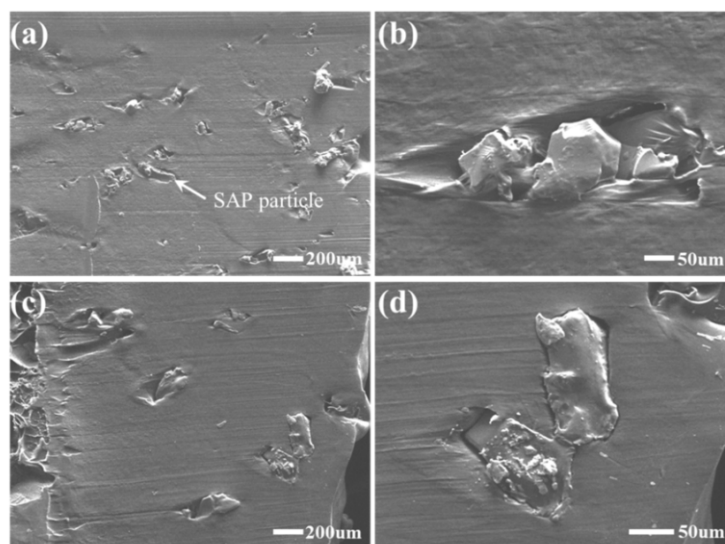


Fig. 4 (a) and (b) Cross-section of PE specimens mixed with 5 wt% small (38-180 μm) SAP particles prepared by thermal extrusion; (c) and (d) Cross-section of PE specimens mixed with 5 wt% big (180-300 μm) SAP particles prepared by thermal extrusion. It can be seen that the SAP particles can survive through the thermal extrusion process with high temperature, high pressure, and high shear stress.

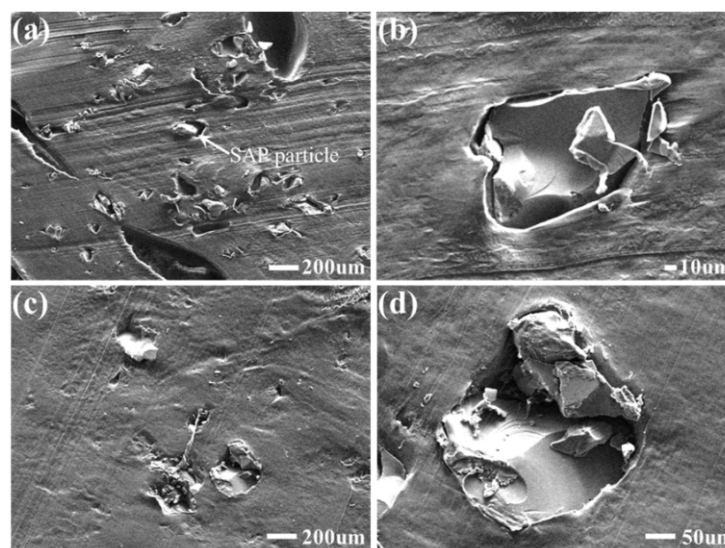


Fig. 5 (a) and (b) Cross-section of PE specimens mixed with 5 wt% small (38-180 μm) SAP particles prepared by hot pressing; (c) and (d) Cross-section of PE specimens mixed with 5 wt% big (180-300 μm) SAP particles prepared by hot pressing. It can be seen that the SAP particles can survive through the hot pressing process.

SAP particles can also be observed for both sizes. The two experiments demonstrate the survivability of the adopted SAP particles through both thermal extrusion and hot pressing. The high stability of the SAP particles through these thermal processes lies in that they are lightly cross-linked polymer. And attributed to the same reason, they kept their original shapes, rather than dissolved in the matrix, during the thermal processes. It is worth noting that the SAP particles and the PE matrix do not bond very well at their interface, as shown in Figs. 4d and 5b, owing to their chemical difference. Consequently, the incorporated SAP particles can be also considered as defects in the PE matrix and compromise the mechanical properties of the matrix.

3.3 Characterization of self-sealing PE

3.3.1 Water penetration test for defect in form of pin-hole

Before tests, defect in the form of pin-hole was generated to the center of specimens, as shown in Fig. 6a for a pure PE plate. Pin-hole with a diameter of about 500 μm can be introduced by piercing the specimens with a needle with a diameter of 0.88 mm. Firstly, pure PE plate was subjected to the water penetration test using device as illustrated in Fig. 1a. Fig. 6b shows the penetrated water through the pin-hole with respect to the testing time. It is observed that water in the container penetrates fast at the beginning and the penetration decreases with the decreased water in the container. It is reasonable since the pressure generated by

the gravity of the water in the container decreases with the increased amount of penetrated water. Finally, about 26 g (26.1 ± 3.1 g) of 50.0 g water penetrates through the pin-hole from the container. Due to the hydrophobicity of the PE matrix, the curve of the water surface in the small hole is protruding. The extra pressure exerted by this curvature to the water according to Laplace Equation can cancel out the pressure generated by the residual water. It is worthy of noting that the penetration of water is very sensitive to external interventions, like shaking or vibration. Nevertheless, this result demonstrates that water can penetrate through the defect in the form of pin-hole easily.

The fabricated self-sealing PE specimens with compositions as shown in Table 2 were also tested using the same device and procedure after the introduction of pin-holes with the same 0.88 mm needle. It can be seen that all the specimens can successfully impede water penetration through the pin-hole for the 1st sealing cycle. For easy comparison, results of the pure specimen and self-sealing specimens with different compositions for the 1st cycle were drawn in Fig. 7. Compared to the penetrated water of about 26 g for the pure specimen, less than 3 g water can penetrate through all these self-sealing specimens. For the self-sealing specimen with 5 wt% SAP particles of size in 38-180 μm , the last drop of water dropped off at around 20-40 s. The swelling of SAP particles, which are embedded in the matrix but partially exposed to the pin-hole, takes time to fully block the pin-hole. Hence, it is

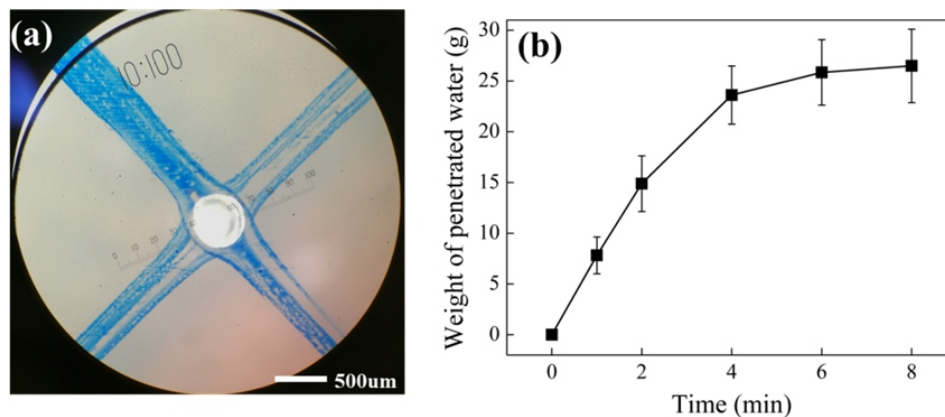


Fig. 6 Defect in form of pin-hole with size about 500 μm introduced by piercing through the pure PE specimen using a needle with diameter of 0.88 mm; and (b) Penetrated water with respect to penetrating duration for pure PE specimen with the centered pin-hole.

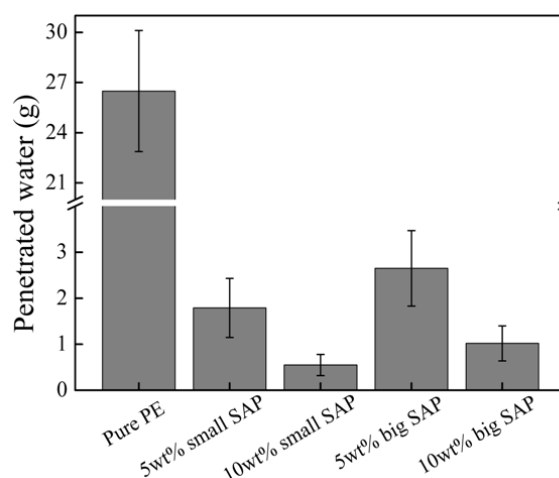


Fig. 7 Comparison of the penetrated water through centered pin-hole in pure PE specimen, self-sealing PE specimens with 5 wt% small SAP particles, 10 wt% small SAP particles, 5 wt% big SAP particles, and 10 wt% big SAP particles, respectively.

reasonable that some of the water penetrates through during the swelling process of SAP particles. It is observed that for the same particle size, the higher the concentration, the less the water penetrates. At higher concentration of incorporated SAP particles, more SAP particles are exposed to the defect. When water flows through defect with more exposed SAP particles, more water is absorbed by them and thus less water penetrates, leading to the higher sealability at higher concentration of SAP. It is also observed that for the same concentration, the smaller the particle size, the better the sealability. This is scientifically reasonable since smaller SAP particles absorb water faster to swell completely and block the defect. In addition, when the concentrations of SAP are the same, a smaller size of individual SAP particle means a larger number of the total particles. As a result, more SAP particles are exposed to the defect. It is concluded that the self-sealing specimen with 10 wt% SAP particles with a size in 38-180 μm gives the best sealability in this investigation. The pin-hole in the specimen with 5 wt% SAP particles of size in 180-300 μm was checked by optical microscope before and after the water penetration test, as shown in Fig. 8. It can be seen that the through-hole is completely sealed by the swollen SAP gels.

Since the absorbed water in SAP gels can evaporate gradually if the water source is removed and the swollen SAP gels are exposed directly to the open air, sealing of the pin-hole disappears when the swollen SAP gels lose the absorbed water and therefore shrinks. It is

necessary to carry out the cycling test to verify the repeatability for the sealability. The sealed specimens were dried at 80 $^{\circ}\text{C}$ for about 12 h to remove the absorbed water in the SAP gels. Interestingly, it is observed that the water penetration was completely avoided for all the cycles for all the specimens with different concentration of SAP particles of different sizes, as shown in Table 2. The reason why the cycling tests show better sealability than the 1st cycle is that the dried SAP particles remain in the pin-hole and it absorbed the penetrated water immediately to block the hole in the cycling tests, while the SAP particles near the pin-hole in the matrix takes time to absorb water and therefore swell for the 1st cycle. Through the observation, it can be concluded that the SAP is suitable for the sealing of defect in the form of pin-hole in the PE matrix.

According to the described phenomena above, besides the investigated self-sealing property, matrix dispersed with the SAP particles has the potential to be adopted as smart rooftop material for constructions. When pre-formed open pores or pin-holes are introduced to this kind of material, the pores/holes with SAP in or around can serve as intelligent switches to control the flow of air and water, attributed to the reversibility of closing and opening of the pores/holes by absorption and desorption of water for multiple times. As a result, it can be utilized for future constructions as the smart rooftop to promote convection of air and moisture during a sunny day and block immediately the penetration of water during a rainy day.

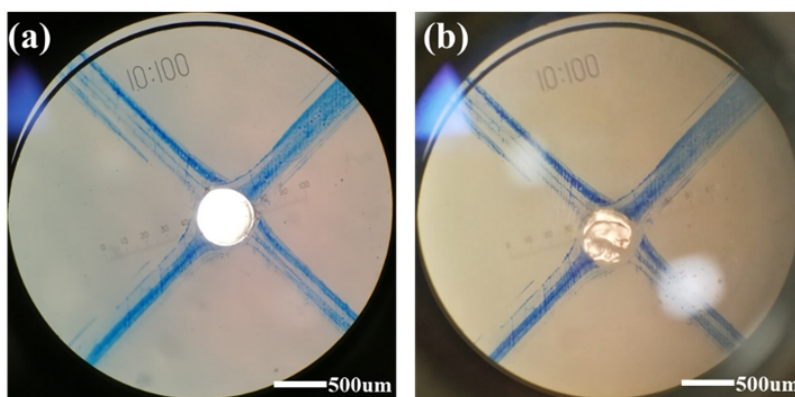


Fig. 8 (a) Pin-hole in self-sealing specimen with 5 wt% SAP particles of size in 180-300 μm before water penetration test; and (b) Sealing of pin-hole by the swollen SAP particles upon their contact with water.

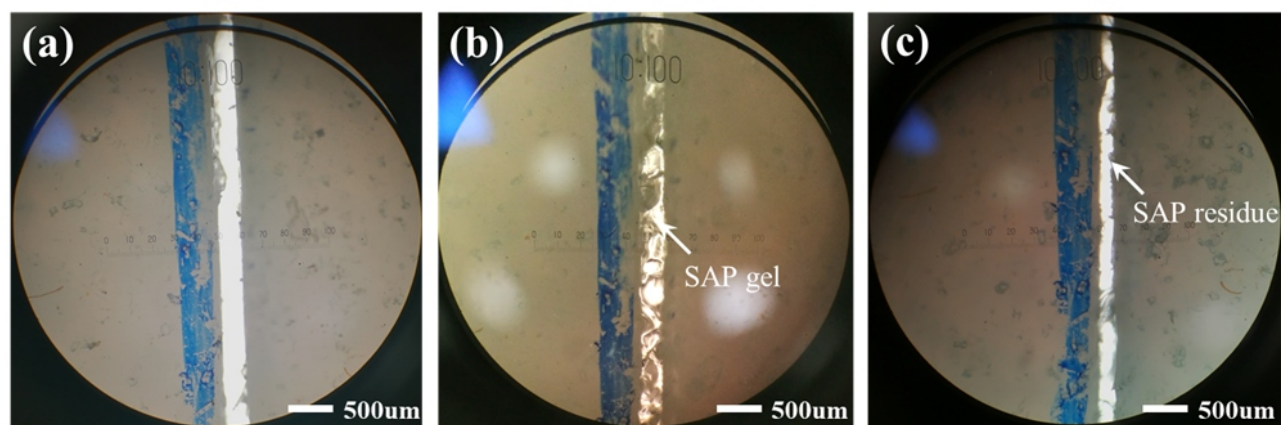


Fig. 9 Self-sealing of manual crack by incorporation of 10 wt% SAP particles with size of 180-300 μm . (a) Crack with length of 20 mm and width of 217 ± 15 μm introduced by cutting the specimen with sharp blade before water penetration test; (b) Sealing of crack by the swollen SAP gels upon their contact with penetrated water; (c) Sealed specimen after being dried at 80 $^{\circ}\text{C}$ for about 12 to remove the absorbed water.

3.3.2 Water penetration test for defect in form of crack

Besides defect in the form of pin-hole, defect in the form of crack with different length and width may appear. In order to verify the sealability for this kind of defect in the self-sealing PE, cracks with different lengths and widths, as shown in Table 3, were introduced to the pure PE and self-sealing PE specimens with 10 wt% SAP particles of size in 38–180 μm by manually cutting the specimens using a sharp blade. For the cracked pure PE specimens, the water in the container was unable to be held and about 37 g (37.5 ± 4.7 g) of 50.0 g water penetrated through during the tests. In contrast, the self-sealing specimens with a similar small crack (138 ± 11 μm) could completely impede the water penetration even for the 1st cycle. However, for the big crack (217 ± 15 μm), about 3.2 g (3.2 ± 1.3 g) water penetrated through the specimen for the 1st cycle during the test, and the last drop fell off in 10–20 s. After the 1st cycle, the complete impedance of water penetration can be obtained. The big crack was imaged before the water penetration test, after the penetration test, and after the drying process at 80 °C for about 12 h, respectively, as shown in Fig. 9. Complete sealing of the crack can be achieved by the added 10 wt% SAP particles with the size of 38–180 μm (Fig. 9b) after the water penetration test. And after the drying process, dried SAP residue can be observed in the crack (Fig. 9c), which is totally different from that before the water penetration test (Fig. 9a). The rapid response to the penetrated water during the following cycling tests results from the SAP residue in the crack.

3.3.3 Water penetration test under extra pressure

Since the PE products might be used in some conditions with higher pressure and the SAP particles turn to soft SAP gel with relatively low strength after absorption of water, it is necessary to test the sealability of this system under elevated pressure. According to the height (about 65 mm) of 50.0 g water in the water container, the generated pressure is only about 0.64 kPa. In order to achieve higher pressure, a modified setup with extra pressure was adopted, as shown in Fig. 1b. After the introduction of pin-holes, self-sealing specimens with 10 wt% SAP particles with the two sizes were subjected to the water penetration tests with elevated pressure. It is observed that self-sealing PE specimen with the small SAP particles (38–180 μm) can only hold the water in the container for about 30 s (less than 1 min) under the extra pressure of about 20.68 kPa (3 psi). After that, water penetrated through the pin-hole very fast. It is interesting to see that the specimen can still hold water after removal of the extra pressure, which means that the swollen SAP gels in the pin-hole with low strength are not flushed away by the pressurized water. Water only penetrates through the small gaps between the swollen SAP gels and the pin-hole or the neighboring SAP gels during the test with extra pressure.

However, for the self-sealing PE with big SAP particles (180–300 μm), it can completely impede the penetration of water for pressure up to 41.36 kPa (6 psi). No further increase of the pressure was allowed because water leaks fast through the gap between the O-ring and the specimen. It can be seen that the big SAP particles are much more suitable for the sealability of PE specimens when extra pressure presents. The better sealability under extra pressure for big SAP particles lies in that the swollen big SAP particles exert higher pressure against the pin-hole compared to the swollen small SAP particles, leading to the higher difficulty for the pressurized water to penetrate through even under higher pressure. The good performance under moderate extra pressure adds value to the conceived smart rooftop made of this kind of material mentioned previously, considering the impact of the falling rain and the generated pressure by the casual water.

4. Conclusions

In this investigation, the possibility of using SAP particles to realize the self-sealing function in polyolefins was explored. Attributed to the high absorbability of water and high thermal stability of the adopted SAP based on cross-linked sodium poly(acrylate), the SAP particles are good candidates as the sealants in polyolefins. Self-sealing PE was fabricated by incorporating the PE matrix with different concentration of SAP particles with different sizes. It is found that all the specimens have good sealability towards defects in the forms of both pin-hole and crack, compared to pure PE. Attributed to the reversibility of absorption and desorption of water for the SAP particles and the left SAP residue in the pin-hole after drying, repeated sealing to defects can be achieved with full sealability. It is observed that for the same particle size, the higher the concentration, the better the sealability, and that for the same concentration of the SAP particles, the smaller the particle, the better the sealability. And finally, although smaller SAP particles can enable better sealability at low pressure, the bigger ones are better for the situation with a higher pressure. Since the adopted SAP is compatible with most polymers including both thermoplastics and thermosets, it can be applied to other polymeric materials to realize the same self-sealing functions. This self-sealing system also opens a window for applications where natural convection of air is preferred but running or flushing water is undesirable.

Conflict of interest

There are no conflicts to declare.

Acknowledgments

We are grateful to Prof Xiao Hu and Dr. Xuelong Chen (MSE@NTU, Singapore), Mr. Suleyman Deveci (Borouge PTE) for their kind help and support. Financial supports from the Start-up Grant from HKUST (R9365), Hong Kong Research Grants Council (Project No. N_HKUST631/18), Borouge PTE (Grand NO. M4061781), and the Science and Technology Planning Project of Guangdong Province (Grant No. 2018A030313264) are also gratefully acknowledged.

References

1. S. R. White, N. R. Sottos, P. H. Geubelle, J. S. Moore, M. R. Kessler, S. R. Sriram, E. N. Brown and S. Viswanathan, *Nature*, 2001, **409**, 794–797.
2. H. Zhang, X. Zhang, C. Bao, X. Li, D. Sun, F. Duan, K. Friedrich and J. Yang, *J. Mater. Chem. A*, 2018, **6**, 24092–24099.
3. H. Lei, S. Wang, D. J. Liaw, Y. Cheng, X. Yang, J. Tan, X. Chen, J. Gu and Y. Zhang, *ACS Macro Letters*, 2019, **8**, 582–587.
4. M. Huang and J. Yang, *J. Mater. Chem.*, 2011, **21**, 11123–11130.
5. H. Zhang and J. Yang, *J. Mater. Chem. A*, 2013, **1**, 12715–12720.
6. M. Samadzadeh, S. H. Boura, M. Peikari, S. M. Kasirih and A. Ashrafi, *Prog. Org. Coat.*, 2010, **68**, 159–164.
7. D. O. Grigoriev, M. F. Haase, N. Fandrich, A. Latnikova and D. G. Shchukin, *Bioinspir. Biomim. Nan.*, 2012, **1**, 101–116.
8. D. G. Shchukin, *Polym. Chem.*, 2013, **4**, 4871–4877.
9. H. Wei, Y. Wang, J. Guo, N. Z. Shen, D. Jiang, X. Zhang, X. Yan, J. Zhu, Q. Wang, L. Shao, H. Lin, S. Wei and Z. Guo, *J. Mater. Chem. A*, 2015, **3**, 469–480.
10. B. A. Beiermann, M. W. Keller and N. R. Sottos, *Smart Mater. Struct.*, 2009, **18**.
11. J. L. Moll, S. R. White and N. R. Sottos, *J. Compos. Mater.*, 2010, **44**, 2573–2585.
12. J. L. Moll, H. H. Jin, C. L. Mangun, S. R. White and N. R. Sottos, *Compos. Sci. Technol.*, 2013, **79**, 15–20.
13. H. Wang, M. Rong and M. Zhang, *Prog. Chem.*, 2010, **22**, 2397–2407.
14. J. Liu, D. Wang, Y. Chen, S. Li and H. Wei, *Adv. Mater. Res.*, 2014, **968**, 44–

- 48.
15. D. Y. Zhu, M. Z. Rong and M. Q. Zhang, *Prog. Polym. Sci.*, 2015, **49-50**, 175-220.
16. H. Zhang, X. Zhang, C. Bao, X. Li, F. Duan, K. Friedrich and J. Yang, *Chem. Mater.*, 2019, **31**, 2611-2618.
17. H. Zhang, P. Wang and J. Yang, *Compos. Sci. Technol.*, 2014, **94**, 23-29.
18. H. Zhang and J. Yang, *Smart Mater. Struct.*, 2014, **23**, 065004.
19. D. Sun, H. Zhang, X. Zhang and J. Yang, *ACS Appl Mater Interfaces*, 2019, **11**, 9621-9628.
20. D. Sun, H. Zhang, X. Z. Tang and J. Yang, *Polymer*, 2016, **91**, 33-40.
21. J. L. Yang, M. W. Keller, J. S. Moore, S. R. White and N. R. Sottos, *Macromolecules*, 2008, **41**, 9650-9655.
22. S. R. White, B. J. Blaiszik, S. L. B. Kramer, S. C. Olugebefola, J. S. Moore and N. R. Sottos, *Am. Sci.*, 2011, **99**, 392-399.
23. M. Q. Zhang and M. Z. Rong, *Self-Healing Polymers and Polymer Composites*, John Wiley & Sons, 2011.
24. D. Y. Zhu, B. Wetzell, A. Noll, M. Z. Rong and M. Q. Zhang, *J. Mater. Chem. A*, 2013, **1**, 7191-7198.
25. D. Y. Zhu, G. S. Cao, W. L. Qiu, M. Z. Rong and M. Q. Zhang, *Polymer*, 2015, **69**, 1-9.
26. D. Y. Zhu, J. W. Guo, G. S. Cao, W. L. Qiu, M. Z. Rong and M. Q. Zhang, *J. Mater. Chem. A*, 2015, **3**, 1858-1862.
27. M. J. Zohuriaan-Mehr and K. Kabiri, *Iran Polym. J.*, 2008, **17**, 451-477.
28. E. Caló and V. V. Khutoryanskiy, *Eur. Polym. J.*, 2015, **65**, 252-267.
29. M. R. Guilherme, F. A. Aouada, A. R. Fajardo, A. F. Martins, A. T. Paulino, M. F. T. Davi, A. F. Rubira and E. C. Muniz, *Eur. Polym. J.*, 2015, **72**, 365-385.
30. H. X. D. Lee, H. S. Wong and N. R. Buenfeld, *Cement Concrete Res.*, 2016, **79**, 194-208.
31. A. Mignon, D. Snoeck, P. Dubruel, S. Van Vlierberghe and N. De Belie, *Materials*, 2017, **10**.
32. B. Craeye, M. Geirnaert and G. De Schutter, *Constr. Build. Mater.*, 2011, **25**, 1-13.
33. V. Mechtcherine, M. Gorges, C. Schroefl, A. Assmann, W. Brameshuber, A. B. Ribeiro, D. Cusson, J. Custodio, E. F. da Silva, K. Ichimiya, S. I. Igarashi, A. Klemm, K. Kovler, A. N. de Mendonca Lopez, P. Lura, N. Van Tuan, H. W. Reinhardt, R. D. Toledo Filho, J. Weiss, M. Wyrzykowski, G. Ye and S. Zhutovsky, *Mater. Struct.*, 2014, **47**, 541-562.
34. S. Oh and Y. C. Choi, *Constr. Build. Mater.*, 2018, **159**, 1-8.
35. H. X. D. Lee, H. S. Wong and N. R. Buenfeld, *Adv. Appl. Ceram.*, 2010, **109**, 296-302.
36. H. X. D. Lee, H. S. Wong and N. R. Buenfeld, *Cement Concrete Comp.*, 2018, **88**, 150-164.
37. A. Mignon, G.-J. Graulus, D. Snoeck, J. Martins, N. De Belie, P. Dubruel and S. Van Vlierberghe, *J. Mater. Sci.*, 2015, **50**, 970-979.
38. A. Mignon, D. Snoeck, D. Schaubroeck, N. Luickx, P. Dubruel, S. Van Vlierberghe and N. De Belie, *React. Funct. Polym.*, 2015, **93**, 68-76.

Publisher's Note Engineered Science Publisher remains neutral with regard to jurisdictional claims in published maps and institutional affiliations.